

Extension of Gkeyll Discontinuous Galerkin Kinetic Code to 2D

Eric Shi ¹ Greg Hammett ² Ammar Hakim ²

¹Princeton University ²PPPL

APS DPP Meeting, 28 Oct 2014

Gkeyll Overview

- Prototype code to explore advanced algorithms for continuum edge gyrokinetic simulation (e.g. edge plasma turbulence)
 - Emphasis on using energy-conserving schemes
- Main code is written in C++
- Lua scripts for simulations

Goal

A robust code capable of running very quickly at coarse velocity space resolution while preserving all conservation laws of gyrokinetic/gyrofluid equations and giving fairly good results.

Background

- Previously, Gkeyll's Poisson bracket solver was formulated for two dimensions ($1x + 1v$ and $2x$)
- Goal of this work is to extend Gkeyll's Poisson bracket solve capabilities to handle general Hamiltonian systems in $2x + 2v$ and $3x + 2v$
- Algorithm (an extension of the work of Liu and Shu¹) conserves energy exactly even with upwinding and is stable in the L_2 norm of the distribution function f
 - Allow distribution function to be discontinuous
 - Hamiltonian is in the continuous subset of space used for f

¹J.-G. Liu and C.-W. Shu. "A High-Order Discontinuous Galerkin Method for 2D Incompressible Flows". In: *Journal of Computational Physics* 160.2 (2000), pp. 577–596. ISSN: 0021-9991.

Evolution Equation

The Poisson bracket operator is defined as

$$\{f, g\} = \frac{\partial f}{\partial z^i} \Pi^{ij} \frac{\partial g}{\partial z^j}.$$

We are interested in solving conservative equations of the form

$$\frac{\partial(\mathcal{J}f)}{\partial t} + \nabla \cdot (\mathcal{J}\alpha f) = 0,$$

where ∇ is the phase-space gradient operator and α is the phase space velocity vector whose components are defined as

$$\alpha_i = \dot{z}^i = \{z^i, H\} = \Pi^{ij} \frac{\partial H}{\partial z^j}.$$

Discontinuous Galerkin Solutions

Discontinuous Galerkin schemes use discontinuous function spaces (usually made of polynomials) to represent the solution.

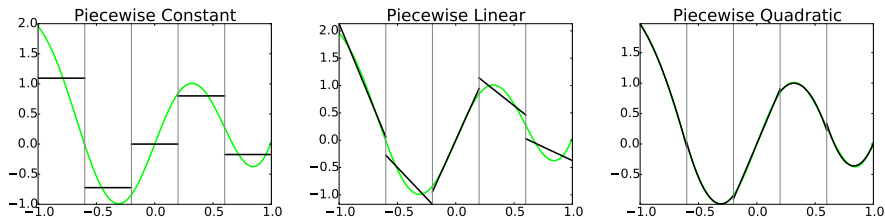


Figure: The best L_2 fit of $x^4 + \sin(5x)$ (green) using piecewise constant (left), linear (center), and quadratic (right) polynomials.

Discretization of the Evolution Equation Using DG

- Introduce a mesh K_j of the domain K .
- Find f_h in the space of discontinuous piecewise polynomials such that for all basis functions ϕ_k , we have

$$f_h(x, y, v_{\parallel}, \mu, t) = \sum_k f_k(t) \phi_k(x, y, v_{\parallel}, \mu)$$
$$\int_{K_j} \mathcal{J}_h \phi_k \frac{\partial f_h}{\partial t} d\mathbf{z} = \int_{K_j} \mathcal{J}_h \nabla \phi_k \cdot \boldsymbol{\alpha}_h f_h d\mathbf{z} - \oint_{\partial K_j} \mathcal{J}_h \phi_k^- \mathbf{n} \cdot \boldsymbol{\alpha}_h \widehat{F} dS$$

Here, $\widehat{F} = \widehat{F}(f_h^+, f_h^-)$ is the consistent numerical flux on surface ∂K_j and \mathcal{J}_h has been taken to be time-independent.

ETG Test Problem Description

- Model problem involves curvature-driven ETG instabilities and turbulence in a local 2D (2x+2v) limit
- Simulation domain is a small box of size $\Delta R \times \Delta R$ on the outer midplane of a tokamak
- Axisymmetry in toroidal direction
- Parallel gradients of f are ignored
- Use set of coordinates $(x, y, v_{\parallel}, \mu)$, where
 - x is the radial coordinate
 - y is the vertical coordinate
- Goals are to reproduce linear growth rate of instability and produce 2D turbulent nonlinear saturation

Physical Parameters Based on Cyclone Base Case²

Symbol	Expression	Value
ΔR	$32\rho_s$	1.819×10^{-3} m
ρ_s	c_s/Ω_{ci}	5.683×10^{-5} m
B_0		1.91 T
a		0.4701 m
R_0		1.313 m
R	$R_0 + 0.5a$	1.548 m
L_T	$R/10$	0.1548 m
n_0		4.992×10^{19} m ⁻³
$T_{i0} = T_{e0}$		2.072 keV

²A. M. Dimits et al. "Comparisons and physics basis of tokamak transport models and turbulence simulations". In: *Physics of Plasmas* 7.3 (2000), pp. 969–983.

Test Problem Equations

$$H_s = \frac{1}{2} m_s v_{\parallel}^2 + \mu B + q_s \phi$$

$$\mu = \frac{m v_{\perp}^2}{2B}$$

$$\Omega_s = \frac{q_s B}{m_s}$$

$$\mathbf{n} = \begin{pmatrix} 0 & -\frac{1}{q_s B_{\parallel}^*} & 0 & 0 \\ \frac{1}{q_s B_{\parallel}^*} & 0 & \frac{B_y^*}{m_s B_{\parallel}^*} & 0 \\ 0 & -\frac{B_y^*}{m_s B_{\parallel}^*} & 0 & 0 \\ 0 & 0 & 0 & 0 \end{pmatrix}$$

$$\mathbf{b} = \hat{z}$$

$$\mathbf{B}^* = \mathbf{B} + \frac{B v_{\parallel}}{\Omega_s} \nabla \times \mathbf{b} \Rightarrow \mathbf{B} - \frac{m_s v_{\parallel}}{q_s X} \hat{y}$$

$$B_{\parallel}^* = \mathbf{b} \cdot \mathbf{B}^* \Rightarrow B$$

$$\mathcal{J} = m_s B_{\parallel}^* \Rightarrow m_s B$$

Potential solved for by assuming adiabatic ions and using quasineutrality:

$$-n_{i0}(x_0) \frac{q_i}{T_{i0}} \phi(x, y, t) = n_e(x, y, t) - n_{i0}(x),$$

where $n_{i0}(x_0)$ is the value of the ion density in the center of the simulation

Grid Resolution and Boundary Conditions

- Initial simulations represent solution using piecewise linear basis functions
 - Plan to investigate use of higher-order polynomials, Maxwellian-weighted basis functions in future
- Boundary conditions:
 - Zero flux BCs in v_{\parallel} and μ on f
 - Periodic BCs in x and y on fluctuating components of ϕ and f

Coordinate	Number of Cells	Minimum	Maximum
x	N_x	R	$R + \Delta R$
y	N_y	$-\Delta R/2$	$\Delta R/2$
v_{\parallel}	$N_{v_{\parallel}}$	$-\min\left(4, 2.5\sqrt{\frac{N_{v_{\parallel}}}{4}}\right) v_{Te}$	$\min\left(4, 2.5\sqrt{\frac{N_{v_{\parallel}}}{4}}\right) v_{Te}$
μ	$N_{\mu} = N_{v_{\parallel}}/2$	0	$\min\left(16, 4\sqrt{\frac{N_{\mu}}{2}}\right) \frac{mv_{Te}^2}{2B_0}$

Initial Conditions

$$f_e(x, y, v_{\parallel}, \mu) = \frac{n_e(x, y)}{[2\pi T_{e0}(x)/m]^{3/2}} \exp\left[-\frac{mv_{\parallel}^2}{2T_{e0}(x)}\right] \exp\left[-\frac{\mu B(x)}{T_{e0}(x)}\right]$$

$$T_{e0}(x, y) = T_{e0} \left(1 - \frac{x - R}{L_T}\right)$$

$$n_{i0}(x) = n_0$$

$$T_{i0}(x) = T_{i0}$$

For linear simulations, we initialize a perturbation with a single k_y mode:

$$n_e(x, y) = n_0 \left[1 + 10^{-3} \frac{\rho_e}{L_T} \cos(k_{y, \min} y)\right].$$

For nonlinear simulations, a spectrum of k_x modes are included:

$$n_e(x, y) = n_0 \left\{1 + 10^{-2} \frac{\rho_e}{L_T} \cos(k_{y, \min} y) \exp\left[\frac{(x - x_0)^2}{2\sigma^2}\right]\right\}, \quad \sigma = \Delta R/4.$$

Linear Dispersion Relation for ITG/ETG in Local ($k_{\parallel} = 0$) Toroidal Limit

The dispersion relation for the system can be derived as³

$$\begin{aligned} -n_{0a} \frac{q_a \phi}{T_a} &= -n_{0s} \frac{q_s \phi}{T_s} \int d^3v F_0 \frac{\omega - \omega_*^T}{\omega - \omega_{dv}} \\ &= -n_{0s} \frac{q_s \phi}{T_s} \left[R_0 \left(\frac{\omega}{\omega_d} \right) + \frac{R}{L_n} R_1 \left(\frac{\omega}{\omega_d} \right) + \frac{R}{L_T} R_2 \left(\frac{\omega}{\omega_d} \right) \right], \end{aligned}$$

where $\omega_*^T = \omega_* [1 + (L_n/L_T)(v_{\parallel}^2/2v_t^2 + \mu B/v_t^2 - 3/2)]$, $\omega_{dv} = \omega_d(v_{\parallel}^2 + \mu B)/v_t^2$, $\omega_d = k_y \rho_e v_t / R$.

Here, the subscript a refers to the adiabatic species and the subscript s refers to the kinetic species.

³M. A. Beer and G. W. Hammett. "Toroidal gyrofluid equations for simulations of tokamak turbulence". In: *Physics of Plasmas* 3.11 (1996), pp. 4046–4064.

Linear Dispersion Relation for ITG/ETG in Local ($k_{\parallel} = 0$) Toroidal Limit

Neglecting FLR effects, the three parts of the ion response function can be written in terms of the plasma dispersion function⁴:

$$R_0(x) = 1 - \frac{x}{2} Z^2 \left(\sqrt{\frac{x}{2}} \right)$$

$$R_1(x) = \frac{1}{2} Z^2 \left(\sqrt{\frac{x}{2}} \right)$$

$$R_2(x) = \left(\frac{x}{2} - \frac{1}{2} \right) Z^2 \left(\sqrt{\frac{x}{2}} \right) + \sqrt{\frac{x}{2}} Z \left(\sqrt{\frac{x}{2}} \right).$$

Using $n_{0a} = n_{0s}$, and $q_a/q_s = -1$, the dispersion relation is

$$0 = D(\omega) = R_0 \left(\frac{\omega}{\omega_d} \right) + \frac{R}{L_n} R_1 \left(\frac{\omega}{\omega_d} \right) + \frac{R}{L_T} R_2 \left(\frac{\omega}{\omega_d} \right) + \frac{T_s}{T_a}.$$

⁴H. Biglari, P. H. Diamond, and M. N. Rosenbluth. "Toroidal ion pressure gradient driven drift instabilities and transport revisited". In: *Physics of Fluids B: Plasma Physics* 1.1 (1989), pp. 109–118.

Linear Growth Rate Tests

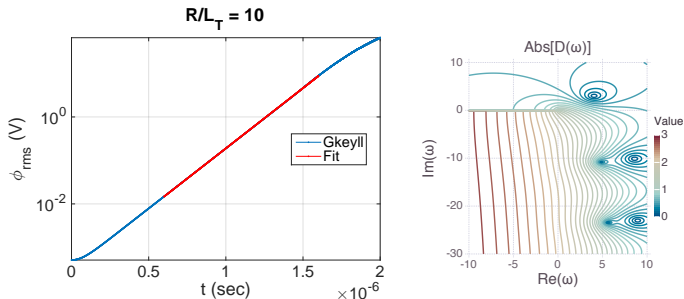


Figure: A linear growth rate for the ETG instability can be extracted from the ϕ_{rms} vs. t plot and compared with the exact value.

For $R/L_n = 0$ using $N_x = 4$, $N_y = 8$, $N_{v_{||}} = 16$, and $N_\mu = 8$:

R/L_T	$\gamma_{sim}/\gamma_{exact}$
20	1.045
10	1.095
5	1.435

Linear Growth Rate: Convergence

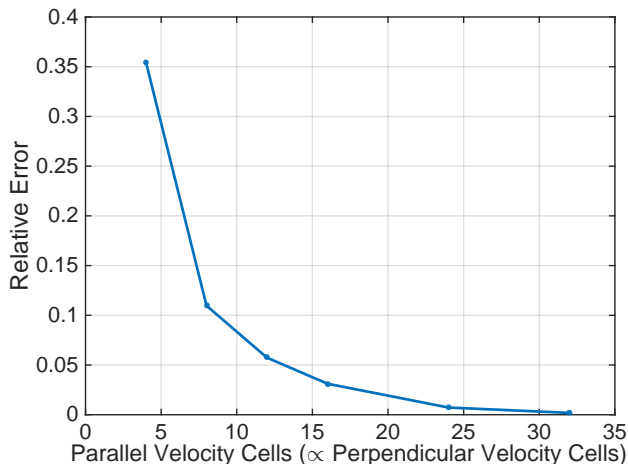


Figure: Convergence of numerical linear growth rate for $R/L_T = 20$ as the number of cells in v_{\parallel} and μ is increased. $N_{\mu} = N_{v_{\parallel}}/2$. Convergence is expected to improve greatly when Maxwellian-weighted basis functions are implemented.

Nonlinear Turbulent Saturation

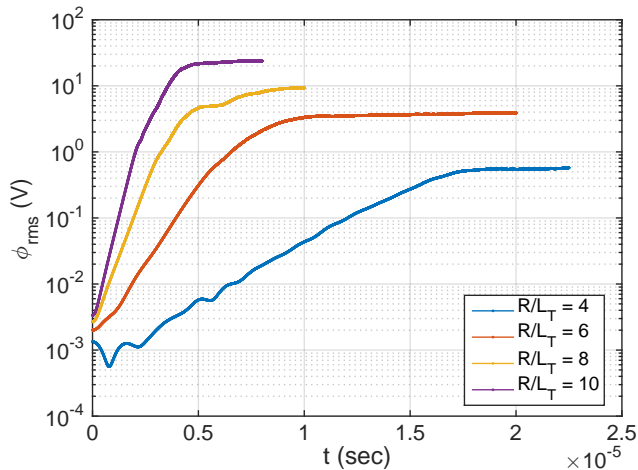


Figure: Plot of ϕ_{rms} vs t for simulations performed at various R/L_T values using $N_X = 8$, $N_Y = 8$, $N_{V_{||}} = 4$, $N_\mu = 2$.

Nonlinear Turbulent Saturation ($R/L_T = 8$)

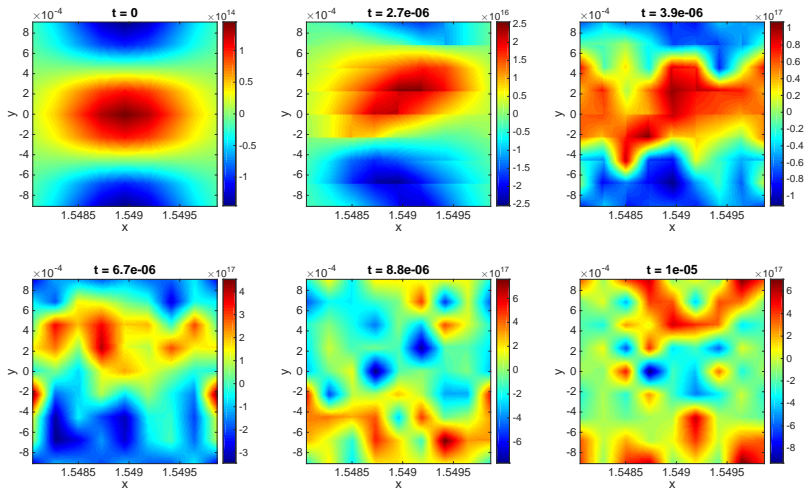


Figure: Plot of $n_e - n_{e0}$ at various times. $N_X = 8$, $N_Y = 8$, $N_{V_{||}} = 4$, $N_{\mu} = 2$.

Nonlinear Turbulent Saturation ($R/L_T = 4$)

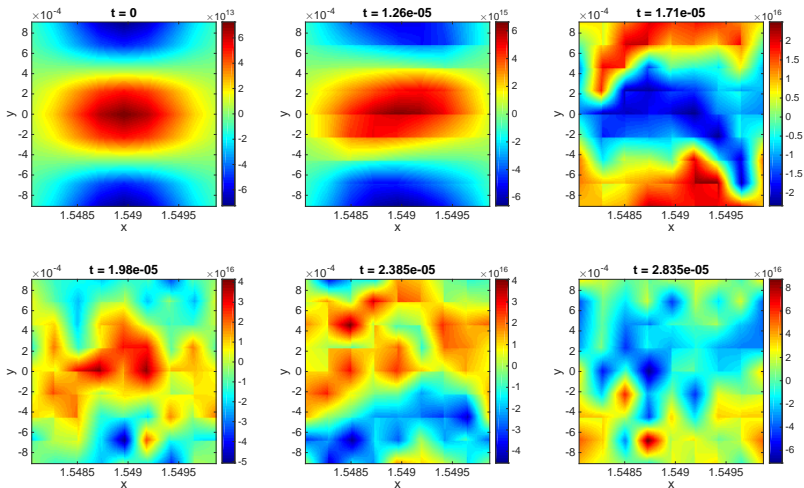


Figure: Plot of $n_e - n_{e0}$ at various times. $N_X = 8$, $N_Y = 8$, $N_{V_{||}} = 4$, $N_{\mu} = 2$.

Conclusions

- We are able to observe linear growth rates that converge to the correct values
- Nonlinear runs look qualitatively reasonable and reach turbulent saturated states
- Future plans:
 - Implement Maxwellian-weighted basis functions in μ and v_{\parallel}
 - Solve Poisson equation for potential
 - Add support for more complicated geometries e.g. non-rectangular and non-uniform meshes
 - Run tests with a third spatial dimension ($3x + 2v$)